JOURNAL OF MATERIALS SCIENCE **36** (2001) 3855–3863

X-ray diffraction from cellulose micro-fibrils in the S2 layers of structurally characterised softwood specimens

K. M. ENTWISTLE
University of Manchester/UMIST, Materials Science Centre, Grosvenor Street, Manchester M1 7HS, UK
E-mail: ken.entwistle@man.ac.uk

N. NAVAREMJAN
Department of Mechanical Engineering, University of Canterbury, Private Bag 4800, Christchurch, New Zealand
E-mail: nava@mech.canterbury.ac.nz

A previous paper (K. M. Entwistle and N. J. Terrill, *J. Mater. Sci* **35** (2000) 1675) reported measurements of the micro-fibril angle of the cellulose fibres in the S2 layers in softwood. The method involved irradiating a specimen with X-rays directed at 45° to the radial and to the transverse direction. The determination of the micro-fibril angle from the distribution of intensity round the (002) diffraction circle assumed an idealised structure in which all the cell walls were oriented precisely in either the radial or the transverse direction. The real cell structure diverges significantly from this ideal. The error involved in assuming the ideal structure has been assessed by making a quantitative image analysis of the length and orientations of the cell walls in a section of the specimen comparable in cross-section to that irradiated by the X-rays. The position of the S2 intensity peaks round the (002) diffraction circle has been calculated and compared with those predicted from the idealised structure. It is demonstrated that the error involved in extracting a value for the micro-fibril angle from the measured intensities using the assumed ideal cell structure of the previous paper (cited above) is not more than one degree in the range of micro-fibril angles 20°–30°. So the approximate analysis is adequate for many purposes.

1. Introduction

In a previous paper [1], a method was presented for the measurement of the micro-fibril angle of the cellulose fibres in the S_2 layers of softwood. This involved mounting the specimen with the wood cell axes vertical and with the X-ray beam directed at 45 degrees to the radial and to the transverse directions. The X-ray intensity distribution around the (002) diffraction circle shows peaks and the azimuth angle between them was used to determine the micro-fibril angle. The analysis that was used to extract values for the micro-fibril angle assumed that the cells were square with all the sides of the squares oriented in the radial and the tangential directions respectively. This assumption implies that there is an equal length of cell wall in the radial and in the transverse directions. An observation of the real cell structure reveals that it diverges significantly from this ideal pattern. Cell corner angles are not all right angles so a proportion of the cell walls do not lie precisely in either the radial or the transverse direction. It is therefore desirable to establish the degree of error introduced into the derivation of the micro-fibril angle from the fact that the real cell structure differs from the idealised form assumed in the analysis described in the earlier paper. To this end, a quantitative image analysis was made of the length and the orientation of the cell walls in a section cut along the R-T plane of specimens for which the (002) diffraction intensity had been measured in the manner previously described. From the distribution of cell wall lengths and of cell wall orientations the distribution of X-ray intensity from the S2 layers round the (002) diffraction circle was calculated. The separation between the calculated positions of the peaks that appear in this intensity distribution was compared with those predicted by the idealised analysis and with the measured peak separations.

2. Measurement of the cell wall geometry

Specimens that had been used for the X-ray determination of the micro-fibril angle were prepared for optical examination by making a fine cut along the R-T plane using a sharp blade. The surface produced gave a clear image of the undistorted cell structure in the optical

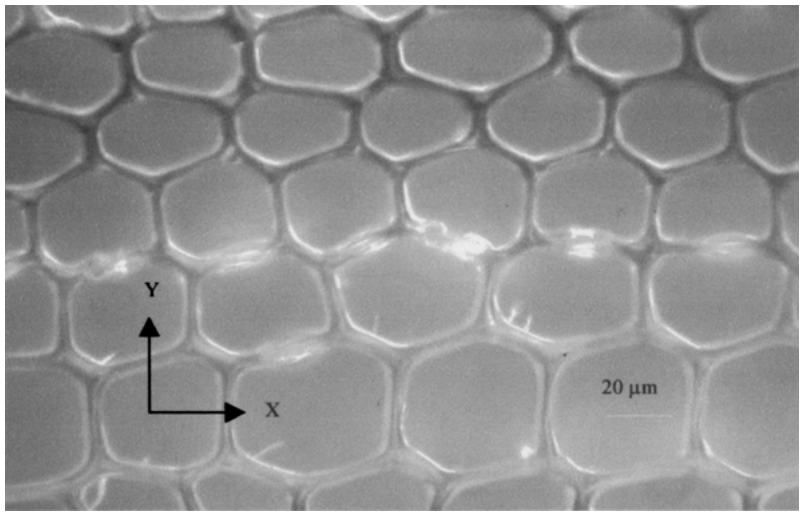

Figure 1 Cell image of R-T plane showing the x–y co-ordinate axes.

image analyser. A typical field of view is presented in Fig. 1.

Images were analysed using a Scion Image Analyser. Five images were analysed for each specimen, four near each corner of the field and one in the centre. More than 1000 cell walls were measured. The length and the orientation of each cell wall were obtained in the following way. Two dimensional co-ordinates were set up in the field of view with the x-direction coinciding with the radial direction and the y-direction oriented in the transverse direction. The x and y co-ordinates of each cell junction were then determined by the image analyser. The length of each cell wall (Δl) and the orientation (θ), relative to the radial direction as zero, were determined by

$$\Delta l = \sqrt{(x_j - x_i)^2 + (y_j - y_i)^2}$$

and

$$\theta = A\tan\left[\frac{y_j - y_i}{x_j - x_i}\right],$$

where (x_i, y_i) and (x_j, y_j) are the co-ordinates of the two ends of an individual cell wall.

The distribution of Δl with θ for one specimen, 940b, is shown in Fig. 2. The angle θ lies between $+90^\circ$ and -90°, that is a range of 180°, because we do not distinguish between cell walls of identical orientation on opposite sides of a single cell. To simplify later analysis we group the individual cell walls together in one degree ranges. To this end we sum the total length of cell wall with values of θ between 0 deg and 1 deg, between 1 deg and 2 deg and so on. Fig. 3 plots the distribution of these one degree range cell lengths as a function of θ. It is interesting to note that, if we regard walls with orientation $\theta = \pm 45$ deg as radial walls and the rest as transverse walls, then the total radial wall length is 3415 μm and the transverse length is 1176 μm. So the radial wall length is about three times that of the transverse walls.

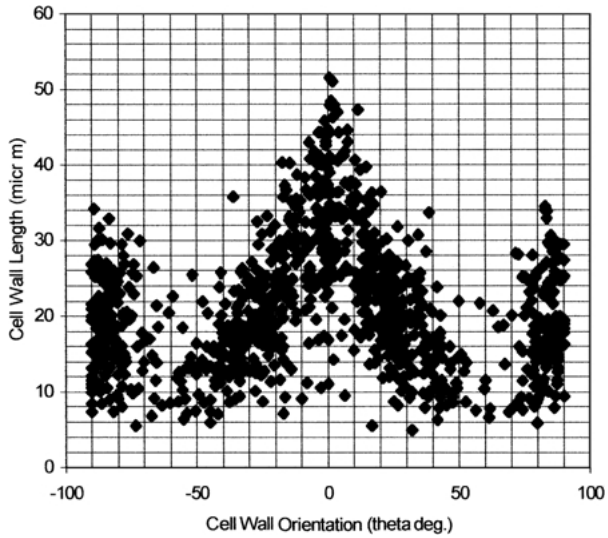

Figure 2 Distribution of individual cell wall lengths specimen 940b.

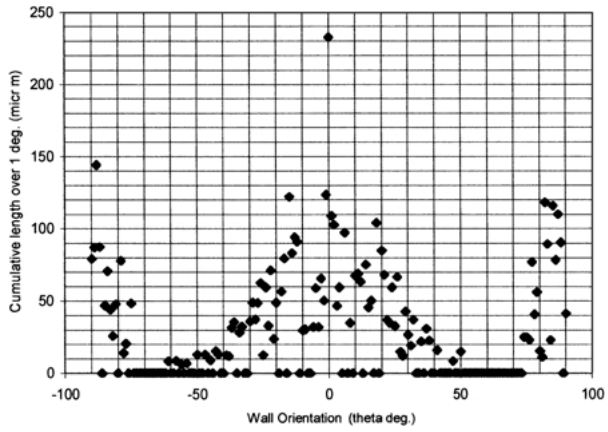

Figure 3 Distribution of total cell wall length over one degree ranges.

3. Calculation of the (002) diffraction intensity distribution

3.1. Diffraction from a single bundle of fibres

We now calculate the distribution of X-ray intensity that would be expected from a specimen with the cell wall geometry defined in Fig. 4. We assume that the

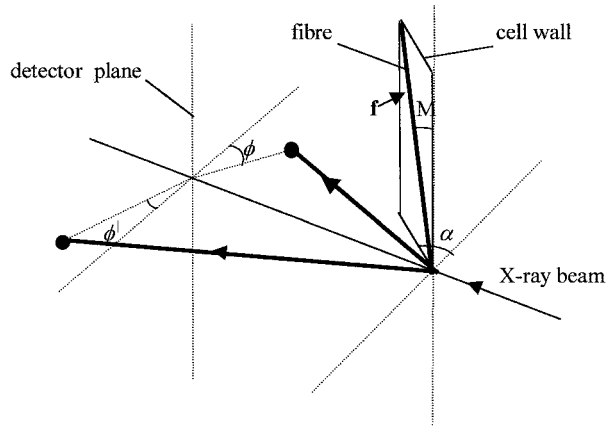

Figure 4 Diffraction geometry for a single bundle of fibres in a cell wall.

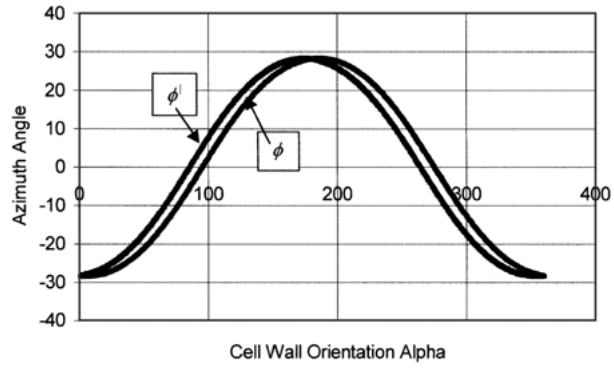

Figure 5 Variation of azimuth angle with cell wall orientation Mo radn.

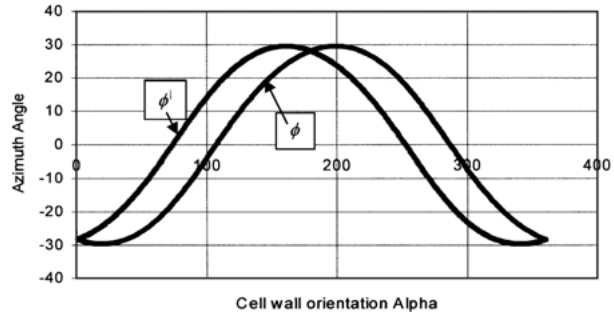

Figure 6 Variation of azimuth angle with cell wall orientation Cr radn.

X-ray diffraction pattern is recorded with the specimen oriented in the X-ray beam with its cell axes vertical and with the specimen rotated about this vertical axis so that the radial direction is at 45 deg to the X-ray beam. This is the diffraction condition used in the method described in the previous paper [1]. In this analysis we shall assume that the radial direction is rotated anti-clockwise (as in Fig. 4) relative to the $\alpha = 0$ orientation. If the specimen were rotated clockwise, the intensity distribution would be the mirror image of that we now calculate. We begin by considering a bundle of parallel cellulose fibres f (Fig. 4) lying in a planar cell wall whose normal is at an angle α to the X-ray beam. The fibres are oriented at an angle M, the micro-fibril angle, to the cell axis direction. We showed previously [1] that the fibres will produce two (002) diffraction spots one at an angle ϕ on the right-hand arc of the diffraction circle and the other at an angle $\phi^{|}$ on the left-hand arc. In general the two spots will not be diametrically opposite.

If we define ϕ as positive if it is anticlockwise and measure ϕ and $\phi^{|}$ from zeros along the nearest equatorial direction, then ϕ and $\phi^{|}$ are given by the following equations:

$$\sin\phi . \cot M = -\{\cos\phi . \cos\alpha + \tan\theta . \sin\alpha\} \quad (1a)$$

$$\sin\phi^{|} . \cot M = -\{\cos\phi^{|} . \cos\alpha - \tan\theta . \sin\alpha\} \quad (1b)$$

where θ is the Bragg angle.

Knowing M, the micro-fibril angle, and θ, the Bragg angle, it is possible to calculate ϕ and $\phi^{|}$ as a function of α, the cell wall orientation. This requires a numerical solution, which was carried out using the Mathcad package. The variation of ϕ and $\phi^{|}$ with α for $M = 28.2$ degrees and $\theta = 5.18$ degrees, corresponding to $Mo\ K\alpha$ radiation, is plotted in Fig. 5. The corresponding curves for $\theta = 16.88$ degrees, corresponding to Cr $K\alpha$ radiation, is plotted in Fig. 6. The two sets of data confirm that, for a given value of α, the azimuth angle for the ϕ and the $\phi^{|}$ diffractions are not equal so the spots are not diametrically opposite. The difference between the angles increases with the radiation wavelength.

3.2. Diffraction from the cell walls

Our concern is with the cellulose fibres in the S2 layers of the cell walls. In an individual cell wall there are two S2 layers in each of which there are two sets of fibres in mirror image orientation. The two sets are identical and can therefore be considered as one set. Fig. 7 illustrates that the diffraction from this set of fibres can be analysed by considering each of them to be a single fibre in a cell wall of the form illustrated in Fig. 4. The fibre f in Fig. 7 is seen to be equivalent the fibre f$^{|}$ which is of the kind illustrated in Fig. 4 in a wall oriented at $(\alpha + \pi)$. The other set in Fig. 7 is similar but in a wall oriented at angle α. The two fibres will give four diffraction spots, two ϕ diffraction spots, on the right hand section of the diffraction circle, and two $\phi^{|}$ diffraction spots, on the left hand section. The location of each spot will be given by Equations 1a and 1b. The spot intensity

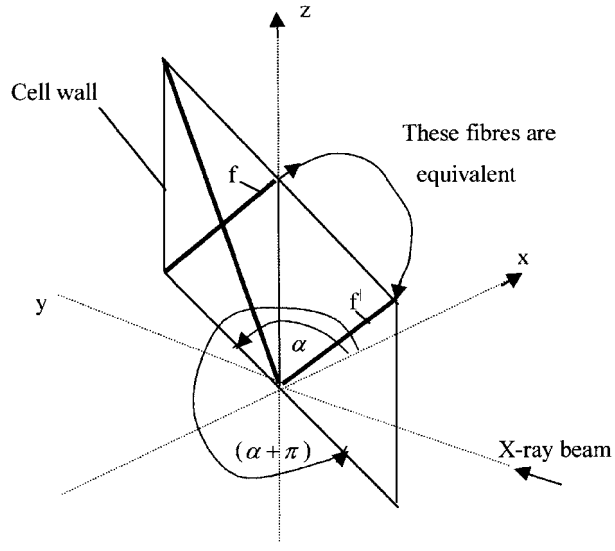

Figure 7 Diagram illustrating that the cellulose fibre f in the cell wall at angle α is equivalent to the fibre f$^{|}$ in the wall at angle $(\alpha + \pi)$.

will be proportional to the length of the cell wall in the R-T plane. In the next section we use these concepts to calculate the total (002) diffraction intensity from all the individual cell walls in the irradiated volume of a specimen that have been characterised by quantitative microscopy.

3.3. Diffraction from the specimen

We now sum the diffraction intensities from all the cell walls in a specimen. We have measured the orientation of all the walls (θ) relative to the radial direction in the wood. For the measurement of micro-fibril angle this direction, $\theta = 0$, lies at 45 deg to the X-ray beam, so the cell wall orientation α as defined in Fig. 4 is

$$\alpha = (\theta + \pi/4).$$

For an individual cell wall of length Δl_i in the R-T plane and with orientation θ relative to the radial direction, there will be four diffraction spots, two of ϕ and two of $\phi^{|}$. The azimuth angles will be derived from Equations 1a and 1b respectively by substituting the known values of M and θ and, in turn, the values

$$\alpha = (\theta + \pi/4) \quad \text{and} \quad \alpha = (\theta + \pi) + \pi/4$$

corresponding to the two sets of fibres in the wall. These azimuth angles are given by the data in Fig. 5.

For the purpose of this comparative exercise, we assume a value for the micro-fibril angle equal to that determined in the previous paper. For the first specimen we analyse, 940b, this is 28.2 deg. The precise value assumed for the micro-fibril angle is not critical in regard to our primary concern, which is the relationship between the predictions from the analysis of the idealised structure and of the real structure. We discuss later the measurement of the micro-fibril angle of specimen 940b.

The individual diffraction spots from a length of cell wall are not sharp because the micro-fibrils in the cellulose fibres wander slightly about the average angle. We can represent the effect of this by assigning a Gaussian distribution to the intensity generated round the (002) diffraction circle. So if ϕ_i is the calculated azimuth angle for (002) diffraction from the single fibre in a wall with orientation α_i then the diffraction intensity ΔI_ϕ at an azimuth angle ϕ is given by

$$\Delta L_\phi = \Delta l_i \exp -\frac{1}{2}\left[\frac{(\phi - \phi_i)}{\sigma_\phi}\right]^2 \qquad (2)$$

where σ_ϕ is the standard deviation of the distribution.

We explore the effect of varying σ_ϕ on the (002) intensity distribution, but we note at this stage that a reasonable value can be derived from Cave's method [2] of determining the micro-fibril angle. He assumes that the edges of the (002) diffraction arcs from the S2 layers of a specimen irradiated in a direction normal to the radial direction are the side of a single Gaussian curve. This spread of intensity derives from the wandering of the orientation of the micro-fibrils in the S2 fibres in cell walls, which in Cave's arrangement are lying in the radial direction in the wood. Cave defines a quantity T which is the separation between the points of intersection of the steepest tangents, drawn to the two edges of the intensity distribution, with the zero intensity line (see Fig. 18). this distance T is shown to be related to the micro-fibril angle by

$$M = 0.62\,T,$$

further, $T - M = 2\sigma$, where σ is the standard deviation of the Gaussian distribution, so it follows that $\sigma = M/3$.

The value of σ_ϕ will depend on the orientation α of the cell wall. The value $M/3$ is for $\alpha = 0$. We can calculate the variation of σ_ϕ with α. The most important value is for $\alpha = 45$ deg which is the orientation of the radial cell walls relative to the X-ray beam for the measurement of the micro-fibril angle. If we let M vary in the range M $\pm M/3$ at $\alpha = 45$ deg we find that the average of ϕ and $\phi^{|}$ varies by $\pm M/4$. For $\alpha = 90$ deg the variation is $\pm M/9$. So reasonable values of σ_ϕ are respectively $M/4$ and $M/9$. Strictly we should calculate σ_ϕ in this way for each value of α, but since the cell walls in the real structures lie dominantly in the directions $\alpha = 45$ deg and $\alpha = 135$ deg we use a value a little less than $\sigma_\phi = M/4$ for all the walls. The chosen value is 5.9 deg but we later explore the effect of quite large variations of σ_ϕ on the position of the intensity peaks. We also calculate in a later section the effect of σ_ϕ on the relation between M and T.

The total (002) diffraction intensity from a specimen is obtained by summing a term like Equation 2 for each wall. To simplify the analysis we have summed the length of the cell walls with orientations in one degree ranges giving 180 values from $\theta = 1$ deg to $\theta = 180$ deg. The result of such a summation is plotted in Fig. 3. If θ_n is the orientation of a one degree set and the sum of the cell wall lengths in the set is Δl_n then the two sets of S2 fibres in these walls will give rise to four diffraction spots centred on the azimuth angles ϕ_{n1}, ϕ_{n2}, $\phi^{|}_{n1}$ and $\phi^{|}_{n2}$. The values of ϕ_{n1} and $\phi^{|}_{n1}$ are obtained by substituting $\alpha = (\pi/4 + \theta_n)$ in Equations 1a and 1b. Correspondingly ϕ_{n2} and $\phi^{|}_{n2}$ are obtained by substituting $\alpha = (\pi/4 + \theta_n) + \pi$ in the same equations. The ϕ values contribute intensity on the right hand side of the pattern around the equator in the detector plane and the $\phi^{|}$ values contribute on the left.

The intensity has a Gaussian distribution around each diffraction spot. So a set of walls of length Δl_n which give a spot at azimuth angle ϕ_{n1} will contribute an intensity ΔI_n which varies with ϕ as

$$\Delta L_n = \Delta l_n \exp -\frac{1}{2}\left[\frac{\phi - \phi_{n1}}{\sigma_\phi}\right]^2 \qquad (2a)$$

ΔI_n was calculated over the range $\phi = \pm 40$ deg from the equatorial point in the detector plane for the 180 values of θ_{n1}. A further 180 values were calculated by substituting in (2a) the values of θ_{n2}. The total intensity in the ϕ region was derived by adding up the intensities for these 360 individual peaks. A similar computation yielded the intensity in the $\phi^{|}$ region.

The summation was carried out in an Excel spreadsheet. Each row of the spreadsheet records the calculated intensity from a single set of fibres in those cell walls that are oriented within a 1 deg band. The first

180 rows list data from fibres in walls with values of α between 1 deg and 180 deg. The second 180 rows, from 181 to 360, are the intensities for diffraction from fibres in the same walls as for the first 180 but in mirror image orientation to the first group. It is explained in the discussion of Fig. 7 that diffraction from these fibres can be analysed by regarding them as geometrically similar to that in Fig. 4 but with values of α 180 deg greater than those for the first group. So the values of α for the second group range from 181 deg to 360 deg. Each row comprises about 100 values of the intensity at values of ϕ ranging from -40 to $+40$ deg. The intensity distribution is calculated from Equation 2. For the first 180 rows, which refer to the diffraction ϕ_1, the value of ϕ_{1n} is derived from Equation 1a, by substituting the appropriate wall orientation α_{1n}. For the rows 181 to 360, which refer to ϕ_2, the values of the azimuth angle ϕ_{n2} is obtained from Equation 1a by substituting the appropriate wall orientation α_{n2}.

The total diffracted intensity at each value of ϕ is obtained by summing the 360 values in each column. This sum of the 360 individual intensity peaks, plotted against ϕ, is the calculated intensity distribution I_ϕ round the (002) diffraction circle. So formally

$$I_\phi = \sum_{\alpha=1}^{\alpha=180} \Delta l_n \exp -\frac{1}{2}\left[\frac{(\phi-\phi_{n1})}{\sigma_\phi}\right]^2 + \sum_{\alpha=181}^{\alpha=360} \Delta l_n \exp -\frac{1}{2}\left[\frac{(\phi-\phi_{n2})}{\sigma_\phi}\right]^2 \quad (3a)$$

The values of Δl_n listed in the spreadsheet are obtained by identifying the value of θ_n corresponding to each value of α_n and looking up the cell wall length in the data graphed in Fig. 3. The sequence of values of Δl_n in the second summation is identical to that in the first because corresponding walls (see Fig. 7) are identical albeit the fibres are in mirror image orientation.

Equation 3a gives the intensity distribution around the equatorial region on the right-hand side of the (002) diffraction circle. In a separate spreadsheet a similar calculation was performed to obtain the intensity distribution $I_{\phi^|}$ in the corresponding region on the left-hand side of the circle. Formally,

$$I_{\phi^|} = \sum_{\alpha_{n1}=1}^{\alpha_{n1}=180} \Delta l_n \exp -\frac{1}{2}\left[\frac{(\phi-\phi^|_{n1})}{\sigma_\phi}\right]^2 + \sum_{\alpha_{n2}=181}^{\alpha_{n2}=360} \Delta l_n \exp -\frac{1}{2}\left[\frac{(\phi-\phi^|_{n2})}{\sigma_\phi}\right]^2 \quad (3b)$$

4. Results

4.1. The idealised square cells

We first present the intensity distribution which is generated by a specimen with cells of square section irradiated in a direction at 45 deg to both the radial and the tangential cell walls. This is the geometry assumed in the analysis of the experimental data in the previous paper. Half of the cell walls will lie at precisely $\alpha = 45$ deg and the other half at $\alpha = 135$ deg. These two sets of cell walls will comprise four sets of fibres corresponding to four values of α_n which are 45, 225, 135 and 315 deg. These will give rise to four diffractions in the ϕ region and four in the $\phi^|$ region. The calculated intensities are shown in Fig. 8 for the ϕ region for a standard deviation σ_ϕ of 1 deg. The peaks in the $\phi^|$ region are identical. Fig. 8 reveals four individual diffraction peaks, which are of equal height because the radial and the tangential walls are of equal length. The four peaks of Fig. 8 and the corresponding four $\phi^|$ peaks are the eight peaks identified in the previous paper [1] but which could not be resolved. The reason for this becomes evident if we increase the standard deviation of the individual intensity distributions. Fig. 9 shows the effect on the intensity distribution in the ϕ range of increasing σ_ϕ to 5.9 deg. Only two peaks appear because the wider spread of the individual peaks has caused adjacent pairs to merge. The effect on the $\phi^|$ distribution is identical. So we conclude that the reason for the failure to observe the eight peaks in the previous investigation is that the spread of intensity due to wandering of the orientation of the micro-fibrils caused adjacent pairs of peaks to merge. It requires a standard deviation of about 4 deg to achieve complete merger.

For Mo Kα radiation, corresponding to a Bragg angle of 5.18 deg, the azimuth angles for the individual peaks are $\pm$ 22.61 deg and $\pm$ 18.92 deg for both ϕ and $\phi^|$. The mean values of the azimuth angles of these adjacent

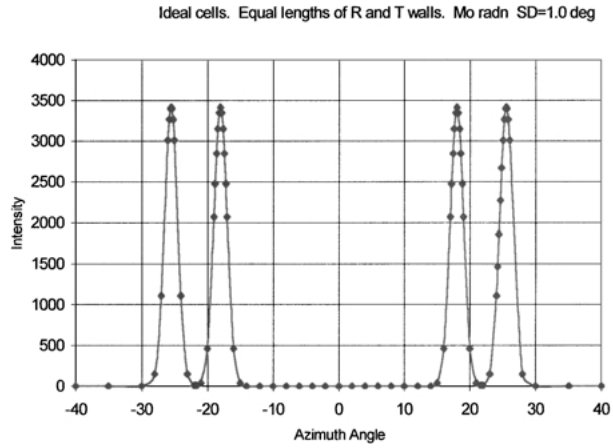

Figure 8 Peak azimuth angles are $\pm$18.92 deg and $\pm$22.61 deg.

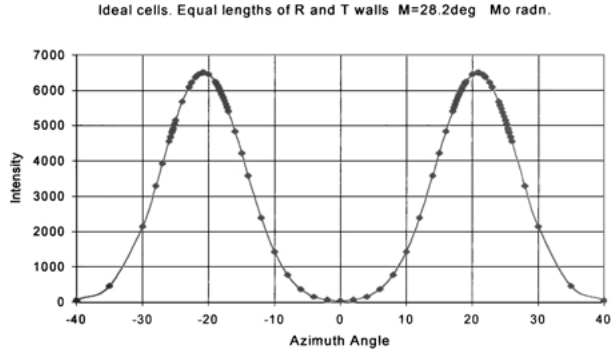

Figure 9 Ideal square cells. With a standard deviation of 5.9 deg the pairs of peaks of Fig. 7 merge. The peak azimuth angles are $\pm$20.75 deg.

pairs are ±20.76 deg which are precisely the azimuth angles at the peak values in Fig. 8.

4.2. Idealised rectangular cells

The distribution of cell wall orientations displayed in Fig. 3 reveals that if we define radial walls as those with $\theta = \pm 45$ deg and the rest as tangential walls, then the length of radial walls in 3415 μm and of tangential walls is 1176 μm. If we assume that all these walls are respectively oriented precisely in the radial ($\theta = 0$) and the tangential ($\theta = 90$ deg) directions, then this corresponds to a cell structure of rectangular cross-section. The individual diffractions for such a structure and for $\sigma_\phi = 1$ deg are shown in Fig. 10 for ϕ and in Fig. 11 for $\phi^|$. The azimuth angles at the peaks are the same as in Fig. 8, that is 18.92 deg and 22.61 deg, but the peak heights differ because of the different R and T cell wall lengths. It should be noted that the order of the R and T intensity peaks is different in the ϕ and in the $\phi^|$ distributions. This arises from the fact, noted in the previous paper, that the ϕ and the $\phi^|$ diffractions from a single fibre do not lie in diametrically opposite positions on the (002) diffraction circle. The effect of this is that, if the standard deviation of the intensity distribution is increased so that pairs of peaks merge, the azimuth angle at the maximum of the merged peaks is different for the ϕ and the $\phi^|$ diffractions. This arises because the taller peaks from diffraction by the radial walls are more widely separated in the ϕ diffractions. Figs 12 and 13 show that if the value of σ_ϕ is increased to 5.9 deg the adjacent pairs of peaks do merge. The azimuth angles at the peaks are ±21.7 deg for ϕ and ±19.8 deg for $\phi^|$. It is interesting to note that the mean value of the azimuth angles for the ϕ and the $\phi^|$ peaks is 20.75 deg which is equal to the mean of the azimuth angles at the two individual peaks that form the merged peak. It is also equal to the azimuth angle for the merged peaks of the idealised square cell structure.

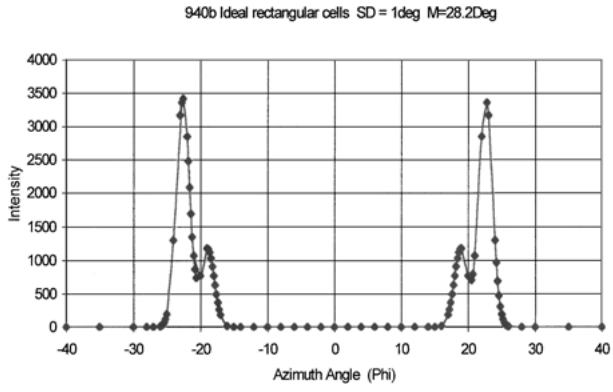

Figure 10 Ideal rectangular cells. R = 3415 μm T = 1176 μm, azimuth angles ϕ. Peak azimuth angles ±18.92 deg ±22.61 deg.

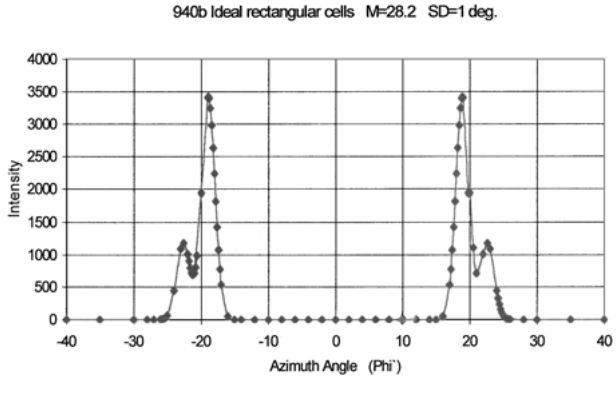

Figure 11 Rectangular cells as in Fig. 9. Azimuth angle $\phi^|$. Peak azimuth angles ±18.92 deg ±22.61 deg.

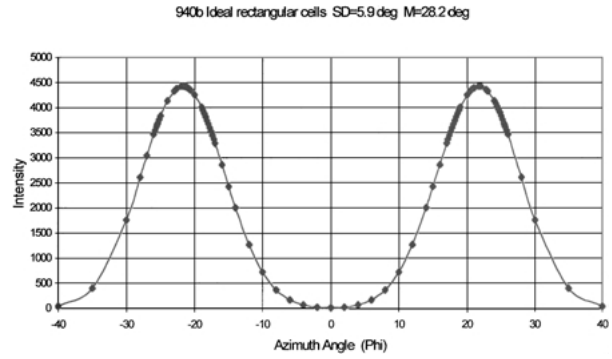

Figure 12 Cells as in Fig. 10. Azimuth angle ϕ. Standard deviation of 5.9 deg causes pairs of peaks in Fig. 10 to merge. Peak azimuth angles ±21.7 deg.

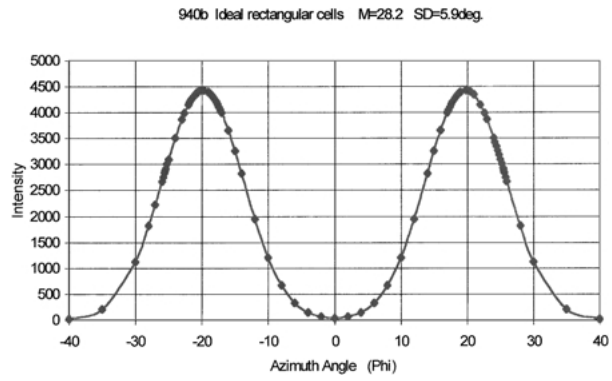

Figure 13 As Fig. 11 but plotting azimuth angles $\phi^|$. Peak azimuth angles ±19.8 deg.

4.3. Diffraction from the real cell structure

We calculate the intensity distribution round the (002) diffraction ring for two specimens.

The first specimen is 940b, for which the distribution of cell wall lengths and orientations is shown in Fig. 3. We use these data to calculate, using Equations 3a and 3b, the intensity within the ϕ and the $\phi^|$ regions between ±40 deg of the equator. The calculated intensities for the ϕ region are plotted in Fig. 14 and for the $\phi^|$ region in Fig. 15. A micro-fibril angle of 28.2 deg is assumed and a Bragg angle of 5.18 deg corresponding to MoKα radiation. The standard deviation σ_ϕ is 5.9 deg.

The azimuth angles at the peaks of the total intensity are $\phi = \pm 21.2$ deg and $\phi^| = \pm 21.8$ deg. The mean of these two angles is ±21.5 deg. We have seen that, if we assume that the cells are square, then the mean value of the ϕ and the $\phi^|$ peaks would be ±20.75 deg. It would have the same value if the cells were rectangular. If, using the assumptions of the previous paper, we had

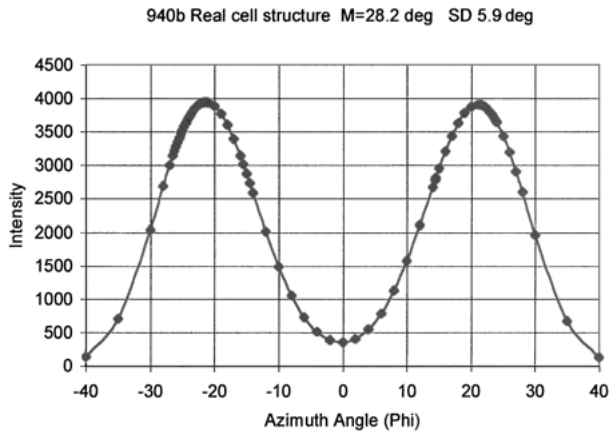

Figure 14 Calculated intensity distribution in the ϕ region for the real cell structure. Peak azimuth angles ± 21.2 deg.

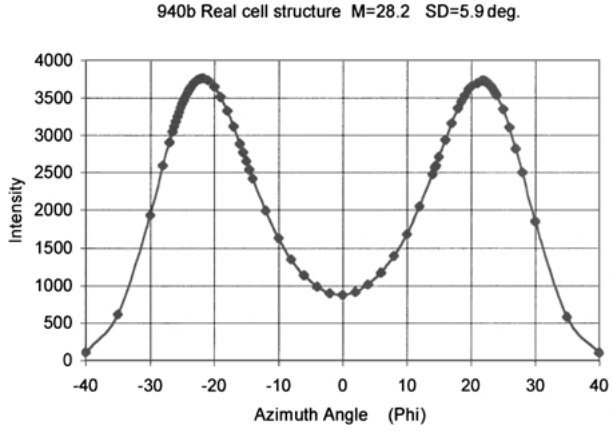

Figure 15 As for Fig. 14 but plotting the intensity in the $\phi^{|}$ region. Peak azimuth angles are ± 21.8 deg.

deduced the micro-fibril angle from an observed mean peak azimuth angle of 21.5 degrees, that is using

$$\mathrm{Tan}\, M = \sqrt{2} * \mathrm{Tan}\phi_{av},$$

we would find $M = 29.12$ deg. The true value assumed in the calculation is 28.18 deg so the error is only 0.94 deg.

We have calculated the effect of varying the standard deviation for the intensity distribution σ_ϕ on the mean azimuth angle for the ϕ and the $\phi^{|}$ peaks. The results are:

Standard deviation σ_ϕ	Mean of the ϕ and $\phi^{|}$ azimuth angles (ϕ_{av})
2.0	± 22.6 deg
4.0	± 21.9 deg
5.9	± 21.5 deg
7.0	± 21.4 deg

Observation of the measured peaks shows that the four pairs of adjacent peaks have merged into four single peaks. Our calculations show that this occurs above a standard deviation of about 4 deg, which places a lower bound on the actual standard deviation. The above table indicates that the effect on ϕ_{av} of variations of σ_ϕ above the value of 4 deg is only 0.5 deg.

We have also calculated the effect of changing the radiation wavelength on the mean angular separation

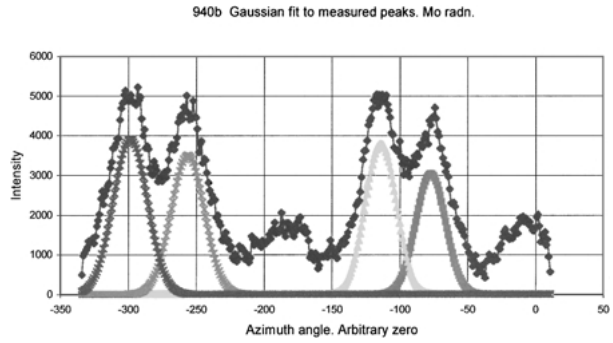

Figure 16 Measured intensity distribution round the (002) diffraction circle. Gaussian curves fitted to peaks. Peak azimuth angles are -298.2 deg, -256.0 deg, -113.8 deg and -76.95 deg.

ϕ_{av} of the ϕ and the $\phi^{|}$ peaks:-

Radiation	Bragg Angle	ϕ_{av}
Mo	5.18 deg	21.5 deg
Cu	11.27 deg	22.2 deg
Cr	16.88 deg	24.0 deg

4.4. Measured azimuth angles

We have measured the position of the peaks on the (002) diffraction circle for specimen 940b using MoKα radiation. The variation of measured intensity with azimuth angle is shown in Fig. 16. The four peaks are evident and Gaussian curves have been fitted to them to establish the peak azimuth angles. The fit gives $\phi = \pm 18.4$ deg and $\phi^{|} = \pm 21.2$ deg so the mean value is 19.8 deg. The relatve heights of the ϕ and the $\phi^{|}$ peaks are affected by specimen absorption; because of the specimen geometry the path lengths of the diffracted beams through the specimen material differ.

The present calculations, based on a determination of the real cell structure of the same specimen, and assuming $M = 28.2$ deg predict $\phi_{av} = 21.5$ deg. A calculation using the same cell structure and assuming $M = 29.4$ deg gave $\phi_{av} = 22.6$ deg. So a change of M of 1.2 deg produces a change of ϕ_{av} of 1.1 deg. Evidently the two changes are nearly equal around this value of M. The ratio of M/ϕ_{av} is 1.31 for both values of M. Using this ratio, the value of M corresponding to the measured value $\phi_{av} = 19.8$ deg is 26.0 deg.

It is interesting to establish the values of the parameters that achieve a fit between the measured peak positions and those calculated from the measured cell wall geometry. The two required parameters are the micro-fibril angle, M, and the standard deviation of the intensity distribution, σ_ϕ. We have seen that the peak positions are not sensitive to values of σ_ϕ above 4 deg. So if we use a value in this range we can regard the micro-fibril angle as the single dependent variable. The analysis in the previous paragraph leads to the conclusion that $M = 26.0$ deg is a good estimate for specimen 940b. To check this conclusion we have put this value into the calculation of ϕ_{av} from the measured cell geometry. The results are

ϕ peaks -19.5 deg and $+19.2$ deg

$\phi^{|}$ peaks -19.85 deg and $+19.6$ deg

These data give a value for ϕ_{av} of 19.5 deg. This agrees well with the measured value of 19.9 deg. The agreement between the positions of the individual peaks is not quite so good but the analysis suggests that $M = 26.0$ deg is a good estimate of the micro-fibril angle. If the observed value of $\phi_{av} = 19.5$ deg had been used to deduce the value of M using the approximate relation of the previous paper a value of 26.6 deg emerges. So the error in using the approximate relation is only 0.6 deg.

A potential source of error in the measurement of the peak positions is mis-orientation of the specimen in the X-ray beam. We can calculate this effect.

With $M = 28.2$ deg, $\sigma_\phi = 5.9$ deg and the specimen oriented with $\theta = 45$ deg, which is the intended orientation, $\phi_{av} = 21.5$ deg. If the specimen is rotated so that ($\theta = 47$ deg to simulate a 2 deg error $\phi_{av} = 21.55$ deg, so the effect is trivial. With $\theta = 55$ deg, that is a 10 deg error, $\phi_{av} = 22.05$ deg so the peak is shifted by 0.5 deg. We conclude therefore that the specimen orientation is not a very critical factor.

4.5. A Second specimen

We have carried out a further comparison on another specimen Ba1 r6. The measured distribution of cell wall lengths is plotted in Fig. 17. It is evident that, as with the previous specimen, walls in the general radial direction dominate. The total radial wall length (in the range $\alpha = \pm 45$ deg) is 26192 μm and the length of transverse walls (the rest) is 13817 μm.

From earlier measurements we assume a micro-fibril angle of 20.2 deg. For MoKα radiation giving a Bragg angle of 5.18 deg we calculate the following values for the average peak azimuth angle:

Assumption	Average peak Micro-fibril Angle ϕ_{av}
Ideal square cells	14.65 deg
Ideal rectangular cells	14.55 deg
R = 26192 μm T = 13817 μm	
Real cells	14.7 deg

It is evident that for this specimen the differences in the predicted values of ϕ_{av} are small. If the calculated value from the real cell structure had been used to derive the microfibril angle using the relation

$$M = A\tan(\sqrt{2} * \tan(\phi_{av}))$$

the value of M is 20.35 deg which compares with the true value of 20.2 deg. So the error is only 0.15 deg.

5. Specimens irradiated normal to the radial direction

It is interesting to calculate the intensity distribution round the (002) diffraction circle for specimens irradiated in a direction normal to one of the principal directions—in this case the radial direction. Cave [2] used this irradiation geometry to measure his parameter T which we have referred to in Section 3.3. We can determine T from our calculated intensity distribution and relate it to the micro-fibril angle M.

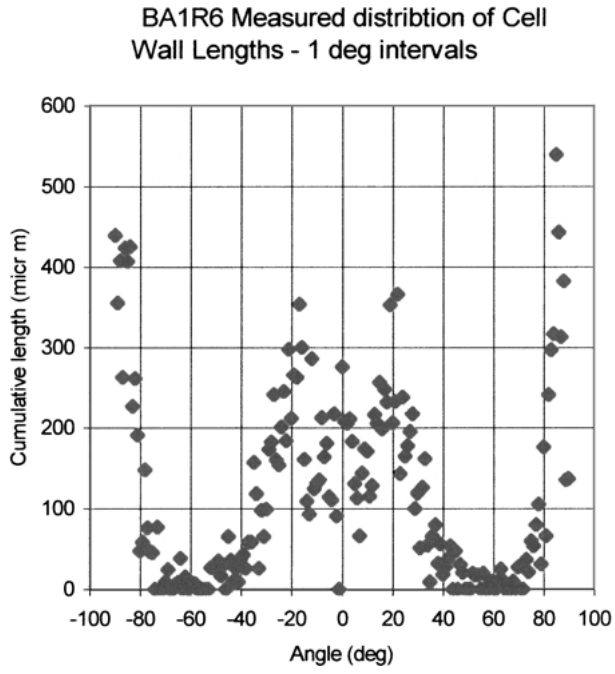

Figure 17 Result of quantitative microscopic determination of the length of cell walls and their orientations within one degree intervals.

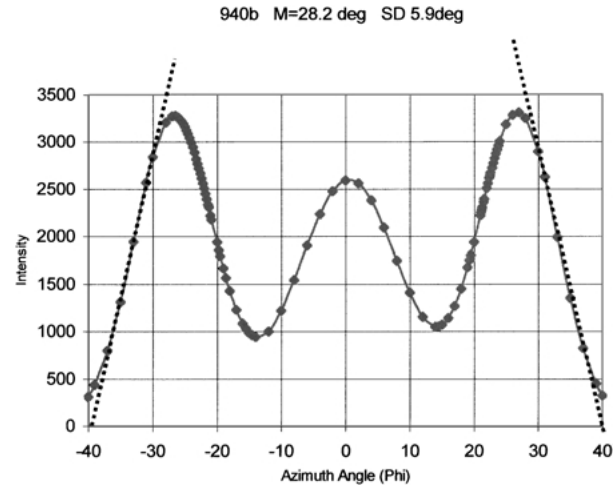

Figure 18 The intensity distribution in the ϕ region for specimen 940b irradiated in a direction perpendicular to the radial direction. The distance between the points of intersection of the dotted tangents with the zero intensity axis is $2T$.

Cave uses the relation

$$M = 0.62T$$

derived from Melan's comparison [3]. We now explore the conditions under which this relation is valid. We calculate the (002) intensity distribution from the measured cell geometry of specimen 940b with the X-ray beam directed normal to the radial direction. Fig. 16 shows the result in the ϕ region for a standard deviation of 5.9 deg. Also shown are the tangents drawn through the steepest part of the edges of the intensity distribution, which yield the value of $2T$. It is 78 deg.

We have repeated the calculations for a range of values of the standard deviation σ_ϕ. The following table lists the values of T in both the ϕ and the $\phi^{|}$ regions. We also list the values of M/T.

σ_ϕ	$T(\phi)$	$\frac{M}{T(\phi)}$	$T(\phi^{\vert})$	$\frac{M}{T(\phi^{\vert})}$
5.9 deg	39.0 deg	0.72	39.7 deg	0.71
7.5 deg	41.9 deg	0.67	42.4 deg	0.65
8.0 deg	43.9 deg	0.64	43.3 deg	0.64
8.5 deg	44.5 deg	0.63	44.2 deg	0.64
9.0 deg	45.4 deg	0.62	45.6 deg	0.62
9.5 deg	46.4 deg	0.61	46.4 deg	0.61

The values of $\frac{M}{T}$ are virtually identical for the ϕ and the $\phi^{\vert}$ regions and fall as σ_ϕ increases. It is evident that Cave's value of $\frac{M}{T} = 0.62$ is achieved at a standard deviation $\sigma_\phi = 9.0$ deg which is a little less than 1/3 of the micro-fibril angle.

6. Conclusions

It is evident from the calculations now described that for real cell structures with micro-fibril angles in the range 20–30 deg the approximate analysis described in the previous paper [1] gives a value of M that is adequate for many purposes.

We summarise the data that supports this conclusion. For the first specimen, 940b, assuming a true micro-fibril angle of 26.0 deg the calculated average peak azimuth angle for the characterised structure was 19.5 deg. If this value had been used to derive the micro-fibril angle using the approximate analysis of the previous paper, that is

$$M = A \tan(\sqrt{2} * \tan(19.5))$$

it yields $M = 26.6$ deg. The true value is 26.0 deg so the error is 0.6 deg.

For the second specimen, Ba1r6, with a true micro-fibril angle of 20.2 deg the calculated average peak azimuth angle is 14.7 deg. The approximate analysis gives a value of $M = 20.35$ deg from this so the error is only 0.15 deg.

We are carrying out similar calculations to those now described to assess the error involved in analysing X-ray small angle scattering patterns assuming that the specimens have the idealised structure.

Acknowledgments

One of the authors (K.M.E.) is grateful to Professor Jeremy Astley for the provision of facilities and stimulus during a period as Visiting Professor in the Department of Mechanical Engineering at the University of Canterbury, New Zealand. The authors are also grateful to Professor Ward Robinson in the Department of Chemistry of the same university for the use of his X-ray facility through Ms. Jan Wakeira.

References

1. K. M. ENTWISTLE and N. J. TERRILL, *J. Mater. Sci.* **35** (2000) 1675.
2. I. D. CAVE, *Forest Products Journal* **16** (1966) 37.
3. B. A. MEYLAN, *ibid.* **17** (1967) 51.

Received 22 November 2000
and accepted 27 February 2001